Attractive Surface Forces Due to Liquid Density Depression

Jan Forsman* and Bo Jönsson

Physical Chemistry 2, Chemical Center, P.O. Box 124, S-221 00 Lund, Sweden

Clifford E. Woodward

School of Chemistry, University College, University of New South Wales, Australian Defence Force Academy, Canberra ACT 2600, Australia

Håkan Wennerström

Physical Chemistry 1, Chemical Center, P.O. Box 124, S-221 00 Lund, Sweden

Received: November 7, 1996; In Final Form: March 12, 1997[⊗]

The force between two inert, planar surfaces in a liquid is discussed, focusing on the effect of the reduction in the fluid density between the surfaces. We use a density functional treatment of the fluid, the results of which are verified by comparison with grand canonical Monte Carlo simulations. Our calculations reveal the existence of an attractive force between the surfaces, which at short and intermediate separations is substantially stronger than that expected from the conventional Hamaker or Lifshitz theories. The source of the extra attraction is the interstitial density depression that results from the requirement of chemical equilibrium between the bulk and the confined fluid at all separations. Given inverse sixth power attractions between fluid molecules, the force between the inert surfaces asymptotically decays as the inverse third power of the separation. However, at short separations it displays a qualitatively different behavior. We also find that the attraction increases with temperature, at constant pressure, and decreases with increasing pressure, at constant temperature, contrary to standard Hamaker theory. These results should lead to a more cautious interpretation of some parameters obtained from fitting experimental surface force curves to, for example, the DLVO expression. Furthermore, in discussions of the molecular mechanism of the hydrophobic attraction, the focus is almost invariably on the short-range directional hydrogen bond, or electrostatic, forces. Our calculations suggest that the density depression mechanism could be as relevant as orientational order.

1. Introduction

There are several mechanisms that can generate a long-ranged force between two surfaces (or particles) in solution.[1,2] For some of these the molecular origin is well understood, and qualitatively correct theories have been developed, which are sometimes also in quantitative agreement with experiments.[3−6] In other cases there are still unclear points in both theory and experiment. The surface force apparatus (SFA)[5] and the osmotic stress technique[7] as well as the more recent atomic force microscope have been of seminal importance for the development of this area and for the elucidation of different contributions to surface forces.

The interaction of two charged surfaces, in the SFA achieved by two crossed mica covered cylinders, has been thorougly investigated, and it has been verified that the DLVO (Dejaguin−Landau−Verwey−Overbeek[3,4]) theory is qualitatively correct for solutions containing monovalent ions. In particular, the long-range part of the repulsive double-layer force decays exponentially, as predicted by theory. Fitting the experimental results obtained at short separation to the DLVO theory is more troublesome, and the determination of, for example, the surface charge density seems less reliable.[8,9] One reason is of course that the Poisson−Boltzmann (PB) approach inherent in the DLVO theory is a mean field approximation, which becomes less justified at high surface charge density or with multivalent ions where correlations start to play a role. The general trend is that the PB approximation predicts too strong a repulsion, leading to an underestimate of the surface charge density. Underestimating the attractive term would of course have a similar effect on the fitted parameters.

The interaction between planar hydrophobic surfaces is strongly attractive. However, it has turned out to be very difficult to experimentally determine the range of the force.[10−17] A survey of the current experimental literature reveals that there is no consensus even on the qualitative features of the distance dependence. This is not the proper place for a detailed discussion of the strengths and weaknesses of different experimental studies. Considering that the experimental situation is not settled, this study is made on the tentative premise that the "true" hydrophobic force has a substantially shorter range (<100 Å) than some experimental studies have indicated. We will in this study discuss a simple mechanism that gives rise to a strongly attractive force, at short and intermediate separations. Elementary theories of surface forces in liquids assume an incompressible liquid giving a simple relation between surface displacement and deplacement of molecules. This is an obvious simplification that can lead to substantial errors. In the present paper we study the consequences for the surface force resulting from depression of the solvent density between the surfaces. This general mechanism is analyzed using a density functional treatment originally formulated by Nordholm and co-workers[18,19] and which is usually referred to as the "generalized van der Waals theory". The accuracy of this theory is evaluated by comparison with grand canonical Monte Carlo simulations from a recent study by Berard *et al.*[20]

The idea of surface forces being modified by density variations induced by the presence of surfaces is not new.

* E-mail address: jan.forsman@fkem2.1th.se

[⊗] Abstract published in *Advance ACS Abstracts,* May 1, 1997.

S1089-5647(96)03726-1 CCC: $14.00

Mitchell et al.[21,22] have previously investigated "structural contributions to Hamaker constants", using integral equation theory. However, their approach is less suited for a study of contributions from a *net* reduction of the density in the slit, since they used asymptotic forms of the integrals. They also invoked a superposition approximation for the total surface−solvent correlation function, when two surfaces were present. Furthermore, their integral equation theory does not predict a gas−liquid phase transition, which is expected to be of importance as the liquid becomes metastable. Thus, their focus was on effects of density structure, rather than density reduction.

2. Hydrophobic Interaction

The strong tendency for apolar solutes to associate in aqueous solution is formally attributed to the "hydrophobic interaction". For small solutes, the magnitude has been carefully quantified both experimentally[23] and via simulations,[24−27] but it has proven difficult to obtain an approximate analytical theory describing the phenomenon. It is clear, however, that the hydrophobic interaction is basically due to the strong cohesion in water, which makes it very unfavorable to generate a cavity where an inert solute can be incorporated. The force between large surfaces, resembling the physical situation in SFA experiments, has also been simulated,[28] but such studies are restricted to rather short separations. The surface free energy of an alkane−water interface is approximately 50 mJ/m^2 at room temperature. Thus, the total free energy change, *i.e.*, the integral of the force in bringing two alkane-covered surfaces into contact in water, should be about 100 mJ/m^2. It is, however, not possible to account for such a high surface tension on the basis of van der Waals forces.[2] Consequently, one should not expect that the force between two hydrophobic surfaces is dominated by the van der Waals force, except asymptotically. A simplified yet physically appealing picture of what happens in the solvent phase between two inert walls can be obtained by balancing bulk and surface free energy contributions. Consider two identical infinite planar surfaces, *S*, separated a distance $\hat{h}$ in a liquid. We denote the interfacial free energy (per unit area) as $\hat{\gamma}_{SL}$, while the surface free energy relative to the vapor phase is $\hat{\gamma}_{SG}$. Generally, for solvophobic surfaces, $\hat{\gamma}_{SL} > \hat{\gamma}_{SG}$,and the surface interactions favor vapor rather than liquid between the walls. Under these conditions there is a possibility of capillary evaporation or cavitation. A simple thermodynamic analysis assuming ideal gas behavior in the vapor shows that confined gas and liquid phases coexist at some separation, $\hat{h}_{crit}$, given by

$$\hat{h}_{crit} = \frac{2(\hat{\gamma}_{SL} - \hat{\gamma}_{SG})}{\hat{P}_B \ln[\hat{P}_B/\hat{P}_{sat}]} \quad (1)$$

where $\hat{P}_{sat}$ is the saturation pressure and $\hat{P}_B$ is the external bulk pressure. For $\hat{h} < \hat{h}_{crit}$, the vapor is the more stable phase. Inserting parameters typical for a hydrocarbon−water surface at $\hat{P}_B = 1$ atm and room temperature, one finds that $\hat{h}_{crit}$ is approximately 1500 Å. This number should be treated with some caution, but it points to a possible source for a long-ranged attractive force between two inert surfaces. Prior to evaporation, there will be a lowering of the average density in the slit.

Our discussion above suggests that the liquid will be metastable below $\hat{h}_{crit}$. Nevertheless, provided the barrier to nucleation is sufficiently large, one can treat the metastable fluid as being at a stable equilibrium. Metastable conditions are quite common in experimental systems,[15] and the free energy functional is able to resolve metastable liquid phases.

3. Theory

3.1. Model. We shall treat a model in which spherical fluid particles are confined by two surfaces. These surfaces are "hydrophobic" (or more correctly "solvophobic") in that there is no attractive interaction with the fluid, only an infinite repulsion at the distance of closest approach. The particle−particle interaction, $\hat{u}(\hat{r})$ is given by the Lennard-Jones potential,

$$\hat{u}(\hat{r}) = 4\epsilon[(\sigma/\hat{r})^{12} - (\sigma/\hat{r})^6] \quad (2)$$

The confined fluid is in equilibrium with a bulk at some chemical potential, $\hat{\mu}_B$. As there is no direct interaction between the surfaces, the force between them is solely due to the action of the intervening fluid. The pressure acting on the walls, due to the solvent, can be written as the negative derivative of the free energy per unit area, $\hat{G}_s(\hat{h})$,

$$\hat{P}_s(\hat{h}) = -\frac{d\hat{G}_s(\hat{h})}{d\hat{h}} \quad (3)$$

The solvation pressure will depend on the bulk chemical potential, which in turn is determined by the bulk fluid density, $\hat{n}_B$, and temperature, $\hat{T}$. The choice of $\hat{T}$ and $\hat{n}_B$ will also determine the surface tension of the liquid.

In the following we will be using *scaled* variables. In the scaled system, all energies are multiplied by the factor $1/\epsilon$ and the temperature is multiplied by k_B/ϵ, where k_B is Boltzmann's constant. Scaled lengths are obtained by dividing by σ. Physical quantities will be distinguished from their scaled counterparts by the "hat" symbol.

3.2. Generalized van der Waals Theory. The generalized van der Waals (gvdW) theory[18,19,29] has been extensively applied to nonuniform fluids. The theory exists in several formulations, and the main difference between them is the length scale over which they are able to resolve fluid structure. In the case of a fluid confined by surfaces, the average density profile will vary most rapidly close to the surface. For a dense hard sphere fluid at a hard surface or a dense Lennard-Jones fluid close to attractive surfaces, one expects an oscillatory density profile. In order to resolve oscillatory profiles, one must use a so-called "fine grained" free energy functional[19] in which nonlocal entropy effects are included. However, in the case of Lennard-Jones particles close to repulsive walls, one expects significantly reduced structure. Further, in this study we are interested in the interaction between surfaces that are separated by distances larger than the typical range of oscillatory structures. Thus it should suffice to use a "coarse grained" free energy functional.[18] These types of functionals are much faster to solve numerically. Using the simplest of the gvdW coarse grained functionals, the free energy per unit area for a particular density profile $n(z)$ can be written as

$$\hat{G}_s[n(z);h] = -T\int_0^h dz\, n(z) \ln\left[\frac{\sigma^3(1-n(z))}{n(z)}\right] + (1/2)\int_0^h dz\, n(z)\int_0^h dz'\, n(z')\,\phi(|z-z'|) - \mu_B\int_0^h dz\, n(z) + P_B h \quad (4)$$

The first term on the right-hand side of eq 4 is the entropy contribution, as estimated by an approximation of the free volume available to hard spheres with an effective diameter equal to σ. The second term is a mean field approximation to the interaction between fluid particles. The final two terms are the separation dependent bulk contributions. The bulk pressure,

P_B, and chemical potential, μ_B, are related to the bulk density, n_B, according to

$$P_B = \frac{Tn_B}{1 - n_B} - \frac{16\pi {n_B}^2}{9} \quad (5)$$

$$\mu_B = -T \ln\left[\frac{\sigma^3(1 - n_B)}{n_B}\right] + \frac{T}{1 - n_B} - \frac{32\pi n_B}{9} \quad (6)$$

The laterally integrated pair potential is given by

$$\phi(z) = \begin{cases} 4\pi[1/5z^{10} - 1/2z^4], & z > 1 \\ -\pi(6/5), & z \le 1 \end{cases} \quad (7)$$

The equilibrium density profile, $n_{eq}(z)$, minimizes G_s and thus satisfies the following integral equation:

$$n(z) = (1 - n(z)) \exp\left[-\frac{n(z)}{1 - n(z)} - 1 - \frac{\int_0^h dz'\, n(z')\phi(|z - z'|) - \mu_B}{T}\right] \quad (8)$$

In this work, eq 8 was solved iteratively, until the maximum absolute value of the functional derivative, $\delta G_s/\delta n(z)$, was less than 5×10^{-6}. We used an integration grid of 0.005 in the z -coordinate. We also performed some calculations using half this grid size, and no difference in any property was obtained. A typical calculation was completed in a few minutes on an ordinary work station. For further details we refer to the following work[18,19,30] and references therein.

The net pressure acting on the surfaces, $P_s(h)$, was evaluated by a discrete numerical differentiation of G_s with respect to h, i.e by using the scaled quantity version of eq 3. The contact theorem for hard walls,[1]

$$P_s(h) = Tn_{eq}(0) - P_B \quad (9)$$

does not apply in the coarse grained versions of the gvdW theory. Interestingly, it does apply for fine grained functionals.

Other mean field approaches have also been used to study nonuniform solvent structure. Of particular relevance to this work is the use of the Cahn−Hillard theory to study oil/water inerfaces by Turkevich et al.[31,32] The Cahn−Hillard theory can be obtained from the gvdW approach by replacing nonlocal terms with a density gradient approximation. Such an approach will be used later to study asymptotic solutions of the gvdW equations.

3.3. Hamaker Theory. In the classical theories of surface forces, due to Lifshitz and Hamaker among others, it is recognized that the interactions between surfaces will be modified by the polarizability of an intervening fluid.[1,33,34] The Hamaker expression for the interaction between the surfaces can be obtained from the gvdW theory by imposing a fixed density for the confined fluid, equal to that of the bulk. The free energy functional can then be solved analytically with the following result:

$$G_{s,Ham}(h) = \pi {n_B}^2\left[\frac{1}{90h^8} - \frac{1}{3h^2}\right] \quad (10)$$

The pressure between surfaces in the Hamaker approximation is then

$$P_{Ham}(h) = 2\pi {n_B}^2\left[\frac{2}{45h^9} - \frac{1}{3h^3}\right] \quad (11)$$

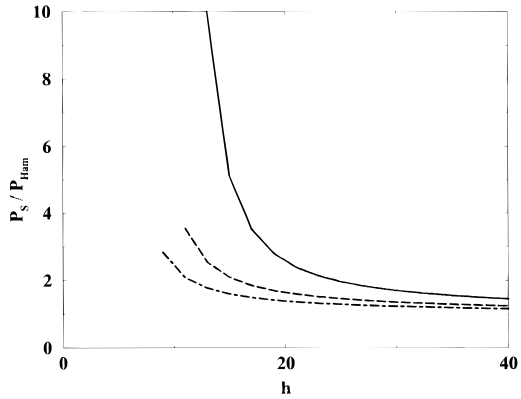

Figure 1. Ratio between the gvdW pressure, P_s from eq 9, and the Hamaker pressure, eq 11, as a function of separation. Temperature and distance are given in reduced units and $P_B = P_{B,ref} = 0.110\,74 \pm 0.000\,03$. Three different temperatures are shown: $T = 0.9$ as a dot-dashed, $T = 1.1$ as a dashed, and $T = 1.3$ as a solid line.

The constraint of a constant density profile for the confined fluid, equal to the bulk value, is a rather drastic approximation, especially close to the surfaces. One of the results of this work is to demonstrate that imposing *chemical equilibrium* between the confined liquid and the bulk leads to a significant modification of P_{Ham}. This was also observed in the simulations of Berard et al., although the emphasis in that work was on the role played by the apparent spinodal separation. Despite the fact that our model incorporates only high-frequency responses, it is clear that the effect we see will impact on the polarizability of the fluid at all frequencies, as these all depend on the fluid density.

4. Results and Discussion

We compared systems at different temperatures and constant bulk pressure. The bulk density was obtained by solving eq 5 at a given temperature. Figure 1 shows the ratio between the gvdW pressure and the Hamaker pressure as a function of separation. As the separation increases, the gvdW and Hamaker results will coincide. This is due to the fact that the average fluid density in the center of the slit will approach the bulk value, with the zones near the walls making an ever diminishing contribution to the free energy of interaction. However, P_s is much more attractive than P_{Ham} at short and intermediate separations. The two pressures can differ by more than an order of magnitude at short separations, and the discrepency can still be as large as 50% at a separation of 40 molecular diameters. One can interpret this additional attractive force (beyond the Hamaker component) as the contribution due to fluid structure. That is, it arises due to the deviation of the confined fluid density away from the bulk value. The Hamaker pressure, P_{Ham}, decays as the inverse third power of separation, but it appears that the structural component of the force decays more quickly, at least at short separations. By studying $P_s - P_{Ham}$, we found that the extra contribution decays algebraically, with the leading long-range term varying as h^{-4}. We present below a perturbation expansion that confirms these findings.

At distances less than the minimum separations depicted on the figures, no stable liquid phase solution to the gvdW equations could be found. At these minimum separations the liquid becomes spinodal. Recently Berard et al. suggested that the spinodal separation could influence the liquid correlation length (even at much larger separations) and that this may account for the long-ranged hydrophobic interaction. We only note here that any such effect (regardless of its importance) will be implicitly included in the gvdW theory.

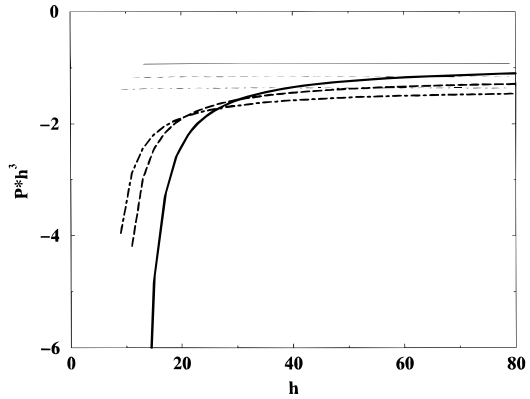

Figure 2. gvdW pressure and the Hamaker pressure multiplied by h^3 as a function of h at $P_B = P_{B,ref}$, for three different reduced temperatures: $T = 0.9$ as a dot-dashed, $T = 1.1$ as a dashed, and $T = 1.3$ as a solid line. The same symbols have been used for the thin horizontal lines representing $h^3 P_{Ham}$.

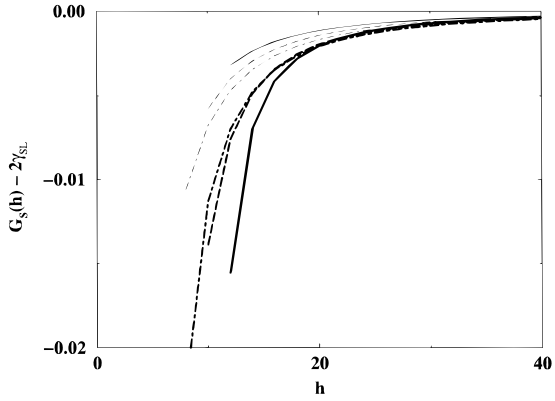

Figure 3. Free energies of interaction, $G_s(h) - 2\gamma_{SL}$, as obtained using the gvdW theory (thick lines) and Hamaker approach (thin lines), respectively. The results for three different reduced temperatures are given: $T = 0.9$ as a dot-dashed, $T = 1.1$ as a dashed, and $T = 1.3$ as a solid line.

The validity of eq 1 was roughly estimated by inserting gvdW values of the required quantities and comparing the predicted critical separation, as found from this expression and gvdW calculations, respectively. Not surprisingly, the agreement is best at high temperatures, where the bulk pressure is closer to the saturation pressure. At $T = 0.9$, eq 1 and gvdW calculations then predict $h_{crit} = 8$ and 21, respectively. At $T = 1.3$, the agreement is much better, with $h_{crit} = 19$ and 27, respectively.

A special feature of the observed attraction is that, for the parameter range investigated, it appears to get larger with increasing temperature. This is opposite the behavior of the Hamaker component. Increasing the temperature at constant bulk pressure leads to a reduction of the bulk density. Equation 11 indicates that this leads to a decrease in P_{Ham}. The additional structural component gives a much more attractive force at higher temperatures, at short to intermediate separations. At larger separations, the structural component has decayed significantly and the total force approaches the Hamaker limit, see Figure 2.

In SFA experiments, which use crossed cylindrical surfaces, the measured force is the net surface free energy of interaction, $G_s(h) - 2\gamma_{SL}$, between flat surfaces (assuming the Derjaguin approximation). In the numerical solution of the gvdW equations, we chose to set $G_s(h) - 2\gamma_{SL}$ equal to zero at $h = 200$, which is large enough to give a very good estimate to the limiting surface tension. The resulting free energy curves are given in Figure 3. Again we see that, as the temperature is increased at constant bulk pressure, the gvdW theory predicts a stronger attraction at shorter separation, in contrast to the Hamaker result. A study of the density profiles obtained from the gvdW theory gives an indication of the mechanism behind this behavior.

Figure 4 displays density profiles, obtained at a fixed separation. It clearly shows a density depletion close to the walls and how, at higher temperatures, the effect of the walls propagates further out. At first sight this result seems counterintuitive. A reduction in the importance of the interactions between particles, as would occur upon raising the temperature, should reduce the depletion effect. Indeed, if the bulk density were to remain fixed and the temperature were to become infinite, there should be no depletion. As we shall see below, however, it is important to keep in mind that, in the systems studied above, the bulk pressure is fixed, not the bulk density. This boundary condition is more consistent with experiments. With the pressure fixed, increasing the temperature increases the correlation length in the liquid, thus leading to an extension

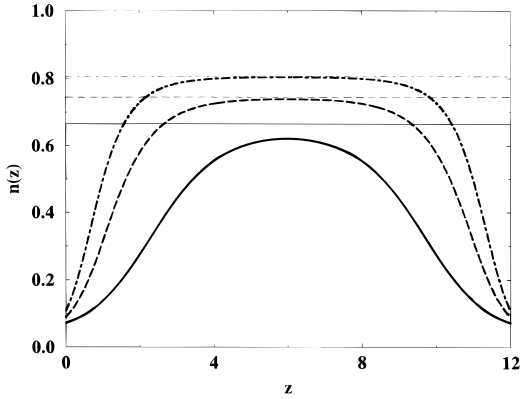

Figure 4. Density profiles for three different temperatures at a reduced separation of $h = 12$ and $P_B = P_{B,ref}$: $T = 0.9$ as a dot-dashed, $T = 1.1$ as a dashed, and $T = 1.3$ as a solid line. The corresponding bulk densities are given as thin horizontal lines.

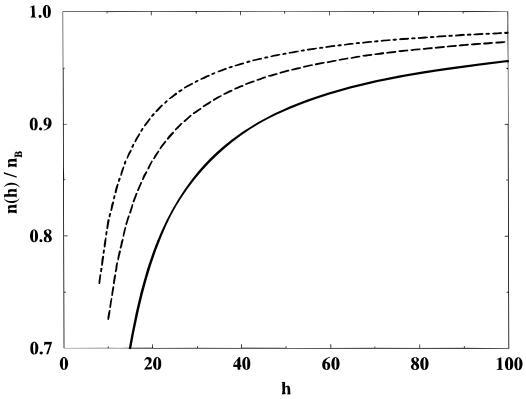

Figure 5. Averaged reduced density as a function of separation for three different temperatures, at $P_B = P_{B,ref}$: $T = 0.9$ as a dot-dashed, $T = 1.1$ as a dashed, and $T = 1.3$ as a solid line.

of the density depleted region toward the middle of the pore. Figure 5 shows how the average density varies with slit width and temperature. Again we see that the effect of the wall increases with temperature.

It is worthwhile pointing out that we also repeated some density profile calculations using fine grained free energy functionals. We found very little difference in the results, provided the comparison was made at the same T/T_c, where T_c is the critical temperature as predicted by the particular version of the theory. This is not surprising, given that the fluid confined by repulsive surfaces does not possess oscillatory

structure. In order to better understand the temperature effect on the fluid density profile, and consequently the free energy of interaction, it is useful to consider a perturbation approximation to the gvdW theory. In particular, we expand the functional $G_s[n(z);h]$ in eq 4 about the bulk density, to second order in $n(z)$. This should be a reasonable approximation for the fluid density profile far from the walls for large h. We show in the Appendix that the leading order expression for the density profile around the center of the slit is given by

$$n(z) \approx n_B - \frac{1}{\lambda}\Psi(z) \tag{12}$$

where $\Psi(z)$ is given by eq 20 and

$$\lambda = \left(\frac{\partial \mu_B}{\partial n_B}\right)_T = \frac{T}{n_B} + \frac{T}{1-n_B} + \frac{T}{(1-n_B)^2} - \frac{32\pi}{9} \tag{13}$$

The function $\Psi(z)$ accounts for the effect of the walls on the density profile. It is positive and decreases monotonically away from the walls, depending on the inverse third power of the distance from the walls. The magnitude of its influence is determined by $1/\lambda$. The correlation length of the bulk fluid is proportional to $\lambda^{-1/2}$. Thus altering conditions so as to increase the correlation length will increase the effect of the walls. For a liquid below the critical temperature, increasing the temperature at constant pressure will move it closer to the bulk liquid/vapor phase boundary. The gvdW equation of state predicts that this leads to an increase in the correlation length, as the liquid phase becomes in some sense "less stable". This explains why, in the example calculations above, the effect of the walls propagates further out at higher temperature. On the other hand, if the bulk fluid is a gas, increasing the temperature at constant pressure will reduce the correlation length, as the fluid moves away from the bulk phase boundary. For the same reason, if the temperature is increased at fixed density in either a bulk gas or liquid, the correlation length decreases. Note that at critical or spinodal conditions in the bulk fluid, one has $\lambda = 0$, and the correlation length becomes infinite.

There have been some attempts to experimentally measure the width of fluid interfaces, and it may be interesting to compare with these. We have attempted to calculate the width of the interface layer against a single surface using the formula[32]

$$\tau = \partial\hat{\gamma}/\partial\hat{P}_B \tag{14}$$

For the pentane/air interface the experimental value[35] is τ = 2.2 Å. From the gvdW theory we obtained a value of 1.6 Å. The calculations employed Lennard-Jones parameters derived by Rodriguez and Freire.[36]

From the perturbation expansion of the gvdW functional the free energy is given by

$$G_s(h) = G_s(n_B,h) + \frac{1}{2}\int_0^h dz\, \Delta n_{eq}(z)\, \Psi(z) \tag{15}$$

where $G_s(n_B,h)$ is the free energy obtained by assuming a constant fluid density, equal to the bulk value. The separation dependent part of $G_s(n_B,h)$ is the Hamaker interaction, eq 10. The second term in eq 15 corrects for fluid structure. We can approximate it with the leading order term for the density, to give

$$G_s(h) = G_s(n_B,h) - \frac{1}{2\lambda}\int_0^h dz\, \Psi(z)^2 \tag{16}$$

The structural correction term contains surface and separation dependent components. The surface component lowers the surface tension term obtained by assuming a constant liquid density profile. One can show that the separation dependent part asymptotically varies as h^{-3} and thus decays faster than the Hamaker component, which goes as h^{-2}. As mentioned earlier, such a decay was indeed obtained from our gvdW calculations, but at separations less than about 40−50 molecular diameters, higher order terms contribute significantly. The structural part of the free energy of interaction also increases with the correlation length. This increase in attraction can more than compensate the reduction in the Hamaker component, as was observed in the examples above. Note that Mitchell et al.,[21] using an entirely different approach, obtained qualitatively identical results, at large separations.

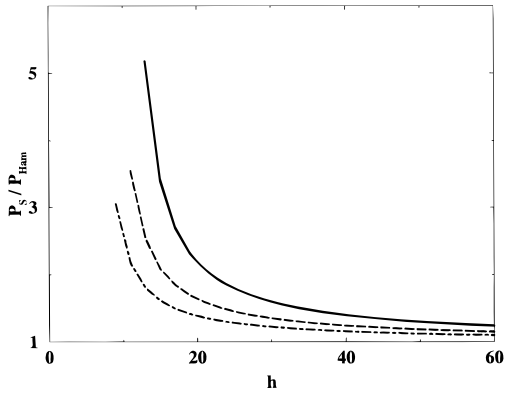

Figure 6. Ratio between the gvdW pressure, P_s from eq 9, and the Hamaker pressure, eq 11, as a function of separation, at $T = 1.1$. Three different bulk pressures are shown: $P_B = 2P_{B,ref}$ as a dot-dashed, $P_B = P_{B,ref}$ as a dashed, and $P_B = P_{B,ref}/2$ as a solid line.

According to the above discussion, lowering the bulk pressure at constant temperature will also move the thermodynamic state of the liquid closer to the phase boundary and may thus increase the attraction at short to moderate separations. This is confirmed in Figure 6, where a 50% reduction of P_B leads to a doubling of the attraction.

An important test of the generalized van der Waals theory is a direct comparison with Monte Carlo or molecular dynamics simulations. Fortunately, a grand canonical Monte Carlo (GCMC) study of a Lennard-Jones liquid between two hard walls has recently been published by Berard et al.[20] We performed test calculations using the gvdW theory with precisely the same parameters and were able to reproduce the MC results within the simulated error bars, Figure 8. The excellent agreement (also found for the density profiles) suggests that one can use the gvdW theory with a great deal of confidence in these types of systems. It should be pointed out that the computation time for the simulations was several orders of magnitude greater than required to solve the gvdW equations.

It would be of considerable interest to attempt to model liquid water and to estimate the effect that the density depression mechanism would have in that system. However, the gvdW theory, at least in any of its simpler versions, is essentially limited to studies of spherical molecules. The approach we take here is to use an effective Lennard-Jones fluid, with some properties similar to that of water. We considered two possible effective models. In the first, we used gvdW results at the same T/T_c and P/P_{sat} as bulk water at room temperature and atmospheric pressure, T_c and P_{sat} being the critical temperature and saturation pressure, respectively. In the second model, the interfacial surface tension, γ, and the bulk isothermal compressibility, κ_T, as given by the gvdW theory were chosen to be similar to those of water. The results using these two models

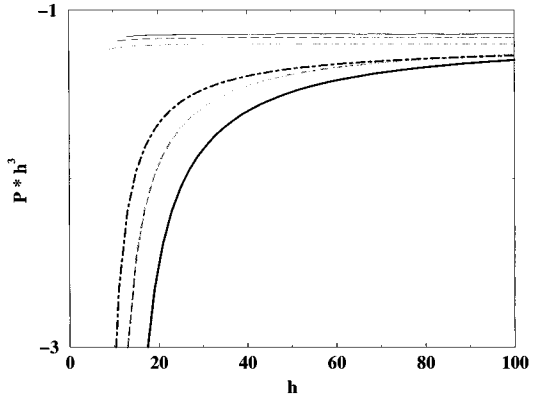

Figure 7. gvdW pressure and the Hamaker pressure multiplied by h^3 as a function of h for three different reduced pressures: $P_B = 2P_{B,ref}$ as a dot-dashed, $P_B = P_{B,ref}$ as a dashed, and $P_B = P_{B,ref}/2$ as a solid line. The same symbols have been used for the thin horizontal lines representing h^3 P_{Ham}.

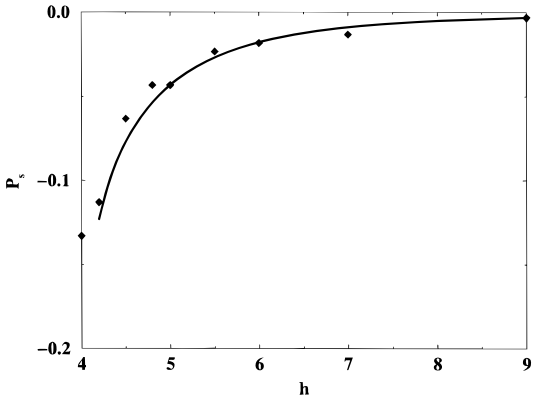

Figure 8. gvdW (solid line) and GCMC (diamonds)[20] data for a Lennard-Jones liquid confined between two hard walls, at $T = 1.0$ and $P_B = 0.44$. In the GCMC simulations, the bulk pressure (and thus the net pressure) is only determined within ± 0.05.

are given in Figure 9. We stress that one could quite validly propose the use of some other effective model, given the nonuniqueness of such a mapping to the spherical fluid. However, the differences that can be expected are, to some extent, indicated in Figure 9. We also calculated the value of τ for these models, using eq 14, and obtained the values 2.5 and 2.9 Å, repectively (assuming a molecular diameter of 3.1 Å). The experimental value for water at the liquid/gas interface is 7.0 Å.[35] A general feature of both models is that a considerable structural component to the pressure is observed at separations below 20−30 molecular diameters, i.e., essentially in the entire "nonretarded" regime.[10]

The possibility of a reduced density in the slit was adressed in a recent experimental study by Kekicheff and Spalla.[37] Their clever approach was to measure the refractive index of the confined fluid from which the mean density could be estimated. Unfortunately, the noise was very large at short separations, so the experiments neither confirm nor disagree with our findings.

5. Conclusions

We have analyzed the effects of fluid density on the interaction between two "solvophobic" surfaces. For hydrocarbon surfaces in water one expects the vapor phase is the most stable form of the liquid at separations less than about 1500 Å. If a vapor cavity does not appear, due to nucleation barriers, there is still a tendency to have a lower than bulk density in the fluid between the surfaces. Using the gvdW theory we analyzed the density profiles between the surfaces and showed that the

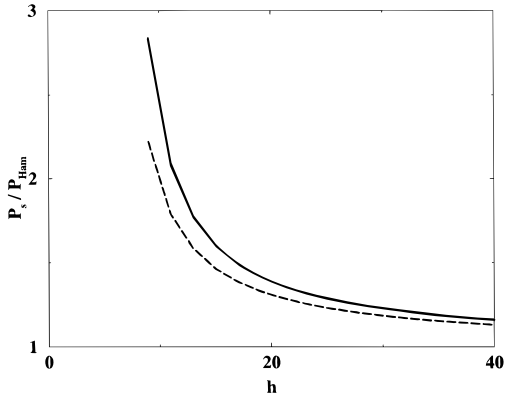

Figure 9. Ratio beweeen the gvdW pressure, P_s, and the Hamaker pressure, P_{Ham}, for model systems, of spherical particles and potentials, with parameters chosen to mimic water confined between hydrophobic surfaces. Two different approaches have been used. The dashed line provides data at the same T/T_c and P/P_{sat} as water at room temperature and atmospheric pressure. Using the isothermal compressibility, $\kappa_T = 54 \times 10^{-11}$ m^3/J of water and a typical surface tension, $\gamma = 51 \times 10^{-3}$ J/m^2, of a water−hydrocarbon interface, the solid line was obtained. As a comparison, we mention that these quantities have, for the state represented by the dashed curve, the following values: $\kappa_T = 28 \times 10^{-11}$ m^3/J and $\gamma = 70 \times 10^{-3}$ J/m^2.

density depletion effect gave rise to significant additional attractive forces between the surfaces. This attractive structural component to the pressure (and free energy) was shown to increase in magnitude as the temperature was increased at constant pressure. This was due to an increase in the correlation length in the liquid, as it was pushed closer to the liquid/vapor phase boundary. A similar effect was observed upon lowering the pressure at constant temperature. It is interesting that this behavior is the opposite of that expected from the classical Hamaker theory.

Our calculations suggest that the density depression contribution to the force between solvophobic surfaces is important at short and possibly intermediate separations. The "hydrophobic interaction" at short range, which is assumed to be extremely important in (for instance) biological systems, may under many circumstances be dominated by the simple density depression mechanism, rather than by some complicated mechanism related to a special feature of water, such as formation of "ice cages" or "hydrogen-bonded networks".

The validity of the gvdW theory was verified by comparison with simulations. The theory proved to be remarkably accurate, presumably due to typically large wavelength fluid structure observed in this system. The numerical labor needed to solve the equations is very modest, and the theory provides a viable alternative to expensive simulation methods.

Appendix

The gvdW free energy functional, eq 4, is expanded about the bulk density to second order in the fluid density, to obtain

$$G_s[n(z);h] = G_s[n_B;h] + \frac{\lambda_0}{2}\int_0^h dz\, \Delta n(z)^2 + \frac{1}{2}\int_0^h dz \int_0^h dz'\, \Delta n(z)\, \Delta n(z')\, \phi(|z - z'|) + \int_0^h dz\, \Delta n(z)\, \Psi(z,h) \quad (17)$$

where

$$\Delta n(z) = n(z) - n_B \quad (18)$$

and

$$\Psi(z,h) = \int_0^h dz'\, n_B \phi(|z - z'|) - \int_{-\infty}^{\infty} dz'\, n_B \phi(|z - z'|) \quad (19)$$

An explicit expression for $\Psi(z,h)$ can be written as

$$\Psi(z,h) = \psi(z) + \psi(h - z) \quad (20)$$

where, for $h \geq 2$,

$$\psi(z) = \begin{cases} -4\pi n_B[1/45z^9 - 1/6z^3], & z > 1 \\ 2\pi n_B[8/9 - 3z/5], & z \leq 1 \end{cases} \quad (21)$$

The quantity λ_0 is the density derivative of the hard sphere part of the bulk chemical potential and is given by

$$\lambda_0 = \frac{T}{n_B} + \frac{T}{(1 - n_B)} + \frac{T}{(1 - n_B)^2} \quad (22)$$

Minimizing $G_s[n(z);h]$ with respect to $n(z)$, one obtains the following relation, which is satisfied by the equilibrium excess density, $\Delta n_{eq}(z)$,

$$\lambda_0 \Delta n(z) + \int_0^h dz'\, \Delta n(z')\, \phi(|z - z'|) + \Psi(z,h) = 0 \quad (23)$$

Substituting the equilibrium density back into eq 17, we obtain

$$\Delta G_s(h) = G_s[n_{eq}(z);h] - G_s[n_B;h] \quad (24)$$

$$= \frac{1}{2} \int_0^h dz\, \Delta n_{eq}(z)\, \Psi(z,h)$$

The left-hand side of eq 24 is the free energy per unit area in excess of the Hamaker contribution. It contains the surface as well as structural component of the total free energy.

Given the form of eq 20, it is possible to express the equilibrium particle density as a superpostion,

$$\Delta n_{eq}(z) = \eta(z) + \eta(h - z) \quad (25)$$

where

$$\lambda_0 \eta(z) + \int_0^h dz'\, \eta(z')\, \phi(|z - z'|) + \psi(z) = 0 \quad (26)$$

This equation can be easily solved numerically; however, some useful asymptotic results are obtained by using a gradient expansion for $\eta(z)$ in the integral. This gives

$$\eta(z) = -\frac{-1}{\lambda_0 + \phi^{(0)}(z,h)} \left[\psi(z) - \sum_{n=1}^{\infty} \frac{d^n \eta(z)}{dz^n} \phi^{(n)}(z,h) \right] \quad (27)$$

where

$$\phi^{(n)}(z,h) = \int_0^h dz'\, (z - z')^n\, \phi(|z - z'|) \quad (28)$$

Given the form of the pair potential, eq 7, the moments $\phi^{(n)}(z,h)$ will diverge in the limit of infinite h, for $n > 2$. This does not mean that there is no solution in this limit but rather that the gradient expansion is only valid over a finite interval. For large h and z, the dominant terms in the divergent moments behave as

$$\phi^{(n)}(z,h) \sim (h - z)^{n-3} - (-z)^{n-3} \quad (29)$$

For $n = 3$, the divergence is logarithmic. Suppose h is large but finite; one can attempt an iterative solution to $\eta(z)$ with zeroth-order approximation,

$$\eta(z) \approx \frac{-\psi(z)}{\lambda_0 + \phi^{(0)}(z,h)} \quad (30)$$

For large h and z near the midplane, $\phi^{(0)}(z,h) \rightarrow -32\pi/9$. Thus in this regime,

$$\eta(z) \approx \frac{-\psi(z)}{\lambda} \quad (31)$$

where λ was given in eq 13. From eq 21, the zeroth-order approximation suggests $\eta(z) \sim z^{-3}$ for large z. Substituting the zeroth-order approximation back into eq 27 and assuming $z \sim o(h)$ generates correction terms of order z^{-6}. Thus the zeroth-order solution is the longest ranged contribution to $\eta(z)$.

References and Notes

(1) Israelachvili, J. *Intermolecular and Surface Forces*, 2nd ed.; Academic Press: London, 1991.
(2) Evans, D. F.; Wennerström, H. *The Colloidal Domain*; VCH Publishers: New York, 1994.
(3) Verwey, E. J. W.; Overbeek, J. T. G. *Theory of the Stability of Lyophobic Colloids*; Elsevier: Amsterdam, 1948.
(4) Derjaguin, B. V.; Landau, L. *Acta Phys. Chim. URSS* **1941**, *14*, 633.
(5) Israelachvili, J. N.; Adams, G. E. *J. Chem. Soc., Faraday Trans 1* **1978**, *74*, 975.
(6) Pashley, R. M. *J. Colloid Interface Sci*. **1981**, *83*, 531.
(7) Parsegian, V. A.; Rand, R. P.; Fuller, N. L.; Rau, D. C. *Methods Enzymol*. **1986**, *127*, 400.
(8) Pashley, R. M.; McGuiggan, P. M.; Ninham, B. W.; Brady, J.; Evans, D. F. *J. Phys. Chem*. **1986**, *90*, 1637.
(9) Kjellander, R.; Marcelja, S. *J. Phys. (Paris)* **1988**, *49*, 1009.
(10) Israelachvili, J. N.; Pashley, R. M. *Nature* **1982**, *300*, 341.
(11) Pashley, R. M.; McGuiggan, P. M.; Ninham, B. W.; Evans, D. F. *Science* **1985**, *229*, 1088.
(12) Claesson, P. M.; Kjellander, R.; Stenius, P.; Christenson, H. K. *J. Chem. Soc., Faraday Trans. 1* **1986**, *82*, 2735.
(13) Claesson, P. M.; Christenson, H. K. *J. Phys. Chem*. **1988**, *92*, 1650.
(14) Parker, J. L.; Cho, D. L.; Claesson, P. *J. Phys. Chem*. **1989**, *93*, 6121.
(15) Christenson, H. K.; Claesson, P. M.; Parker, J. L. *J. Phys. Chem*. **1992**, *96*, 6725.
(16) Parker, J. L.; Claesson, P. M. *Langmuir* **1994**, *10*, 635.
(17) Wood, J.; Sharma, R. *Langmuir* **1995**, *11*, 4797.
(18) Nordholm, S.; Haymet, A. D. J. *Aust. J. Chem*. **1980**, *33*, 2013.
(19) Nordholm, S.; Johnson, M.; Freasier, B. C. *Aust. J. Chem*. **1980**, *33*, 2139.
(20) Berard, D. R.; Attard, P.; Patey, G. N. *J. Chem. Phys.* **1992**, *98*, 7236.
(21) Mitchell, D. J.; Ninham, B. W.; Pailthorpe, B. A. *J. Chem. Soc., Faraday Trans 2* **1978**, *74*, 1098.
(22) Mitchell, D. J.; Ninham, B. W.; Pailthorpe, B. A. *J. Colloid Interface Sci*. **1978**, *64*, 194.
(23) Tanford, C. *The Hydrophobic Effect*; John Wiley: New York, 1980.
(24) Pangali, C.; Rao, M.; Berne, B. J. *J. Chem. Phys.* **1979**, *71*, 2975.
(25) Smith, D. E.; Haymet, A. D. *J. Chem. Phys.* **1993**, *98*, 6445.
(26) Forsman, J.; Jönsson, B. *J. Chem. Phys*. **1994**, *101*, 5116.
(27) Berne, B. J.; Wallqvist, A. *J. Phys. Chem*. **1995**, *99*, 2893.
(28) Forsman, J.; Jönsson, B.; Woodward, C. E. *J. Phys. Chem*. **1996**, *100*, 15005.
(29) Tarazona, P.; Evans, R. *Mol. Phys*. **1984**, *52*, 847.
(30) Freasier, B. C.; Nordholm, S. *J. Chem. Phys*. **1983**, *79*, 431.
(31) Turkevich, L. A.; Mann, J. A. *Langmuir* **1990**, *6*, 445.
(32) Turkevich, L. A.; Man,n J. A. *Langmuir* **1990**, *6*, 457.
(33) Hamaker, H. C. *Physica* **1937**, *4*, 1058.
(34) Lifshitz, E. M. *Soviet Phys. JETP* **1956**, *2*, 73.
(35) Vavruch, I. *J. Colloid Interface Sci.* **1995**, *169*, 249.
(36) Rodriguez, A. L.; Freire, J. J. *Mol. Phys*. **1988**, *63*, 591.
(37) Kekicheff, P.; Spalla, O. *Langmuir* **1994**, *10*, 1584.